Research Article

LSD1 Demethylase Inhibition Prevents Cardiac Fibrosis in Both Ischemic and Congenital Diseases in Mice and Pig Models

Denis Arnaud[1], Virginie Lambert[2], David Benoîst[3], Amandine Martin[4], François Roubertie[4], Jean Gauthier[5], Michel Pucéat[1*]

Abstract

Fibrosis is part of a clinical burden in cardiovascular diseases. The pathological process has been the subject of intensive research with still mitigated therapeutic options. Recently chromatin modifiers have turned out to be potential drugs to modulate fibrosis. Here, in order to address the question of pharmacological inhibition of fibrosis, we used both a mouse model of myocardial infarction with left ventricular fibrosis and a more clinically relevant pig model of right ventricular failure featuring interstitial fibrosis. Treatment of these diseased animal models with an inhibitor of the Lysine Demethylase 1 (LSD1) significantly prevented both left and right ventricular failure in both the mouse and the pig, respectively. This was revealed by a significant recovery of left ventricular function post-myocardial infarction in the mouse and a limitation of remodeling of the pig right ventricle, thus preserving its function. Fibrosis was significantly decreased in both mouse and pig hearts, which likely account for improvement in ventricular function.

We thus provide evidence of the beneficial effect of LSD1 inhibitors in cardiac fibrosis and of the use of such drugs to preserve ventricular function in both ischemic and congenital heart diseases.

Keywords: Fibrosis; Epigenetic modifier; Epithelial-to-mesenchymal transition

Introduction

Cardiovascular diseases remain responsible for a large majority of morbidity and mortality in the vast majority of the world [1]. In both ischemic diseases mostly affecting the left ventricle and in congenital diseases with right ventricular failure often due to ventricular overload and/or overpressure, myocytes cannot ensure any longer their function and die. The death of diseased myocytes is compensated by fibroblasts which when activated together with pericytes rapidly convert into myofibroblasts. The later express and secrete many proteins of the extracellular matrix including smooth muscle actin, periostin, PDGF receptors α and β, collagen 1a1, and fibronectin, which triggers a pathophysiological process so called fibrosis [2]. First adaptative, fibrosis then leads to severe functional defects including deficient contractility and conduction disorders.

Fibrosis often represents the final stage of numerous diseases including cardiovascular, lung and kidney diseases. Despite the tremendous literature on fibrosis, few therapies have been approved at present to target cardiac fibrosis [3].

Affiliation:

[1]Aix-Marseille University, INSERM U1263, INRAE U1260, Centre CardioVasculaire et Nutrition (C2VN), Marseille, France

[2]Institut Mutualiste Montsouris, Paris

[3]Liryc the Electrophysiology and Heart Modelling Institute, Pessac-Bordeaux, France

[4]Department of Congenital Cardiac Surgery, Bordeaux University, Pessac- Bordeaux,

[5]Arythmus, Marseille

*Corresponding author:
Michel Pucéat, Aix-Marseille University, INSERM U1263, INRAE U1260, Centre CardioVasculaire et Nutrition (C2VN), Marseille, France

Recently, studies including epigenetics approaches, uncovered bromo domain and extra-terminal domain (BET) inhibitors as potential anti-fibrotic agents [4,5] through a TGFβ dependent manner [6], a pathway targeted by inhibitors or antibodies in many clinical trials with still mitigated results.

Acetylation of proteins has been also proposed to play a role in cardiac fibrosis [7] making deacetylase potential drugs to alleviate fibrosis. More recently epitranscritomics has been involved in the fibrosis process and related to epigenetics [8]. A very recent paper reported that an HDAC inibitor used in a mouse model of myocardial infarction alleviated inflammation and fibrosis through an inhibition of LSD1 [9].

A novel approach largely used in oncology is emerging for cardiac fibrosis: the CAR T-cell therapy. Fibroblast Activated Protein (FAP) being among the most upregulated membrane protein in activated fibroblast, FAP CAR T-cells were engineered and infused to mouse injured heart. They could decrease fibrosis [10,11].

Interestingly, biological pathways targeted in the treatment of cardiac fibrosis are also targeted in oncology to limit metastasis. Both pathological phenomenon share the same biological process: namely the epithelio-to-mesenchymal transition (EMT).

The epigenetic modifier LSD1 (lysine-specific demethylase 1) plays a crucial role in the formation of metastasis and LSD1 inhibitor prevents the phenomenon by blocking EMT(12). This leads to the development of many LSD1 inhibitors used in clinical trials to target metastasis [13] .

TGFβ-induced fibrosis in skin, lung, liver, and kidney in mouse models was blocked by the formation of LSD1/NR4A1 complex on profibrotic gene regulatory modules [14].

We also reported that inhibition of LSD1 at neonatal stage, prevented fibrosis in a genetic mouse model of dilated cardiomyopathy, i.e., a laminopathy [15].

LSD1 expression is increased in patients featuring dilated cardiomyopathy as well as in mouse model of pressure overload-induced fibrosis. Knock-down of LSD1 in fibroblasts prevented fibrosis and improved ventricular function in a mouse model [16].

Here, we tested LSD1 inhibitors on the development of fibrosis in both mouse models of left myocardial infarction and in a more clinically relevant pig model of right ventricular failure. Using tissue histology and echocardiography, we found that LSD1 inhibitors significantly prevented fibrosis and improved ventricular function in both mice and pigs.

Materials and Methods

Mice: 6-8 weeks male mice (OF1) are housed in cages with environmental enrichment (tunel and kraft paper) and filterring covers with 12h light/12h dark cycle. They were fed ad libidum with a diet including 25% crude protein, 4% Fat, 39.5% carbohydrate, 3.3% crude fibers and 10% neutral detergent fibers suplemented with vitamins. After surgery, mice were isolated in specific ventilated caging system (one mouse/cage) with an improved environmental enrichment and fed with a SAFE® A03 diet.

They were subjected to surgery to perform left coronary ligation.Mice were anesthetized using a mixture of ketamine (71.5 mg/kg) and xylazine (14.5 mg/kg) via intraperitoneal injection. Bupremorphine (0.1 mg/Kg) and carprofen (5 mg/Kg) were given as analgesic. The chest wall was shaved. Drops of lidocaine (21.33 mg/ml) were added on the skin before opening the chest.

Surgery to lead to permanent (occlusion of the artery with a definite ligature) or transient (ligature released after 30 min) left coronary artery was performed as previously published [17].

Atipamezole (0.5mg/Kg), sulfadomethoxin (30 mg/Kg) were given post-surgery. All surgeries were performed in Charles-River laboratories (Les Oncins, Saint Germain Nuelles, France) by veterinary surgeons. All drugs for mice were purchased from Med'vet (France).

Back to the laboratory mice were left for recovery for 10 days post-surgery, monitored by echocardiography (and scored with an ejection fraction below 35%) to normalize the different experimental groups. 90% of mice survived after 2 weeks. The mice were then treated or not (5 mice) by GSK-LSD1 (n=7) (Sigma-Aldrich, France SML1072) 1.5 mg/kg, a reversible LSD1 inhibitor, a dose selected from data obtained in clinical trials in oncology or losartan (n=4) (5 mg/Kg, provided by SANOFI France) by gavage for 3 weeks 3 times/week. SP-2509 (SANOFI, France) a reversible LSD1 inhibitor was also used at 30 mg/Kg.

Mice were weighted every day. No difference of weight was observed between groups (Supplementary Figure 1).

Doppler ultrasound transthoracic echocardiography

Echocardiography was performed 5 weeks post-surgery using an Affiniti 50 (Philips) and a 18-MHz probe. Mice were anesthetized with 4% isoflurane and maintained with 1 to 1.5% isoflurane. Ventricular contractility was monitored using M-mode by positioning the M-mode cursor within the mitral inflow stream pre-recorded by Doppler mode.

Histology and immunofluorescence analysis

After heart explantation from pigs, several around 1 cm3 blocks were cut from the free wall of the right ventricle and were freeze-clamped in liquid nitrogen. Blocks embedded in OCT were then cut in 10 μm sections. Different sections from each block were fixed in PFA 4% and then stained. Adult mouse were fixed in 4% paraformaldehyde overnight at 4°C, then dehydrated with a series of ethanol washes,

and embedded in paraffin. The blocks were sectioned at a thickness of 8 μm. The tissue was rehydratated and sections were stained with eosin and hematoxylin (Sigma-Aldrich, France, 318906 and H3136, respectively) and Sirius Red to stain collagen (Sigma-Aldrich, France Direct Red 80 365548) according to the manufacturer's instructions. At least a total of 100 images/block were acquired with a scanner (Zeiss axioscan). Staining intensity and area of red staining were measured using ImageJ (NIH, Bethesda, MD) for histology images and IMARIS (Oxford instruments) for immunosfluorescence images. We first used the ImageJ plugin Color Deconvolution to separate channels. Then the images were converted into grays scale images and inverted. The stained areas were then segmented using thresholding. Thresholded pixels were normalized to foreground color. The segmented areas were then measured.

Mouse heart sections were also treated with xylene and alcohol to remove paraffin, and after a step of antigen retrieval were stained for anti-smooth muscle actin (SMA, Abcam ab5694), anti-periostin Abcam ab14041) and dapi (DNA). An Alexa-conjuated secondary antibody was used (ThermoFisher Scientific, France Donkey anti-Rabbit IgG, (H+L) Alexa Fluor™ 568 Cat # A10042) SMA+ cells were scored using IMARIS software in at least 3 sections per heart. In IMARIS , we first selected the channel used for SMA staining. Then we used the surface tool and next the mask option (thresholding using the image display) which created a new masking channel. The surface of interest was then displayed in the statistical tab.

Pig Surgery

All experiments were carried out according to the European Community guiding principles in animal experimentation. Four 2 months Landrace male piglets underwent surgery mimicking repaired te-tralogy of Fallot as previously described [18]. Pigs were premedicated by an intra-muscular injec-tion of ketamine (20 mg/kg together with Acepromazine 0.1 mg/kg. Anesthesia was induced with an bolus of Propofol (1-2 mg/kg) after establishment of a venous line. Orotracheal intubation and maintenance of anesthesia was performed with an air/oxygen mixture (50/50) and Isoflurane 1.5-3%. If necessary, 2 additional anesthesia protocols were used: (i) a continuous infusion of propofol or (ii) a continuous infusion of ketamine together with midazolam. Under general anes-thesia, through a left thoracotomy approach, a side-biting vascular clamp was longitudinally set across the pulmonary valve annulus without obstruction of the RV outflow tract. A pulmonary valve leaflet was excised and the pulmonary infundibulum, annulus, and trunk were enlarged by a 2-cm-long, elliptically shaped polytetrafluoroethylene patch to ensure the loss of valve integrity. This chronic pulmonary valve regurgitation led to RV volume overload. Branch pulmonary arterial ob-struction is not uncommon after surgical correction of TOF related to native hypoplasia or

surgical complications and is known to increase pulmonary valve regurgitation. In our model, RV pressure overload was achieved by pulmonary artery banding, made of umbilical tape, placed around the artery truncus and secured for a final diameter of approximately 1 cm to ensure progressive pul-monary stenosis with animal maturation.

Buprenorphine at 30μg/kg, was given to pigs twice a day from the end of the procedure for 3 days. Anti-inflammatory agent (Flunixin 2mg/kg/IM) was given for 5 days. Antibiotics was used 12 hours post-surgery (Cefalexin 10 mg/kg). Analgesics were also given as follows Buprénor-phine 30μg/kg/IM Sufentanil 1 à 2 µg/kg/h Lidocaïne on scar 3mg/kg/h, Ketamine 0,6mg/kg/h Fentanyl 4,5µg/kg/h. All drugs were injected in spine muscle. All drugs for pigs were purchased from Med'vet (France).

Awakening of the animal was carried out under thermal homeostasis. After waking up, the animals were monitored by a competent person every day and were housed (at least 2 pigs together/room) in an enriched environment including balls and toys in rooms with controlled temperature, light and hygrometry. The piglets (up to 45 days old) and pigs were fed with a diet including 13% crude protein, 5.6% crude fat, 6,% cellulose, 3.6% crude ashes, 0.52% methionine and 0.6% lysine, vitamins E, D3 and A, and oligo-elements including Cupper, iron, zinc, manganese, iodine and selenium, and 15.2% crude protein, 2.1% crude fat, 7.1% cellulose, 4.8% crude ashes, hy-droxy-methionine, vitamins D3 and A, and oligo-elements including Cupper, iron, zinc, manganese, iodine and selenium, respectively. After 5 months (median: 158 ± 48 days), the combined pressure and volume overloaded RV leads to its contractile failure. Pigs were treated with the LSD1 inhibitor (1.5 mg/Kg) incorporated in the food 3 weeks (median 21 days) after the surgery for a median duration of 30 days.

At the end of the protocol, pigs wre anesthetized as described before and a ventricular fibrillation was induced to trigger euthanasia.

Pig Heart Echocardiography

RV function was evaluated in all animals at each step of experimental procedure at baseline before rTOF surgery, at and at 5 months at the end of study.

Echocardiography was performed on closed-chest animals under general anesthesia in the dorsal decubitus position. We used a commercially available Vivid E9 ultrasound machine (GE Medical Systems, Milwaukee, WI) equipped with a 2.5-MHz transducer. The values of all echocardiographic parameters were obtained as the average value of three consecutive cardiac cycles during transient apnea and analyzed on a comprehensive workstation (EchoPAC 110.1.2; GE Vingmed Ultrasound, Horten, Norway). Standard parameters of RV function such as Fraction of Area Change, Tricuspid

Annular Systolic Plane Excursion (TAPSE), S'wave on TDI) as well as myocardial strain (longitudinal global and free wall strain) were monitored.

LSD1 enzymatic activity. LSD1 was assayed using a kit (P-3078-48 Epigentek) according to the manufacturer.

Statistics. Data were analyzed by Graphpad Prism using two-ways anova or T-tests.

Institutional Review Board Statement

All animal experiments were carried out according to the European Community guiding principles n°2010/63/UE, law 2013-118 1st February 2013 in animal experimentation. The study was reviewed by ethical committees of the Aix-Marseille and Bordeaux Universities and agreements were obtained from the French Ministère de l'Agriculture.

Results

We first used a mouse model of myocardial infarction (MI) following permanent or transient left coronary ligature. Six to eight months old mice were treated with 1.5mg GSK-LSD1/Kg or with 5mg/Kg Losartan 10 days post-surgery for 3 weeks, 3 days/week. Echocardiography was performed before surgery, ten days post-surgery and after 3 weeks to assess left ventricular function. Mice were then euthanized. The heart was explanted, and sectioned for histological monitoring.

Figure 1A shows that myocardial infarction was severe. The ventricular wall was significantly thinner in mice subjected to MI than under negative control condition (defined as healthy mice with no MI and no treatment) as revealed by eosin/hematoxylin staining. Sirius red staining also revealed an extended fibrosis in mice with MI while it was absent in control mice. While Losartan partially limited the extent of fibrosis (Figure 1A,B) in mice subjected to MI, GSK-LSD1 that diminished the enzymatic activity of the demethylase (Supplementary Figure 2) even significantly further decreased the impact of the pathophysiological process. This was accompanied by a thickening of the left ventricular wall that was more prominent in GSK-LSD1-treated mice than in losartan-treated mice (Figure 1C).The reversible LSD1 inhibitor SP 2509 used at 30mg/Kg also significantly decreased fibrosis in the post-MI hearts to the same extent as GSK-LSD1 (Figure S3).
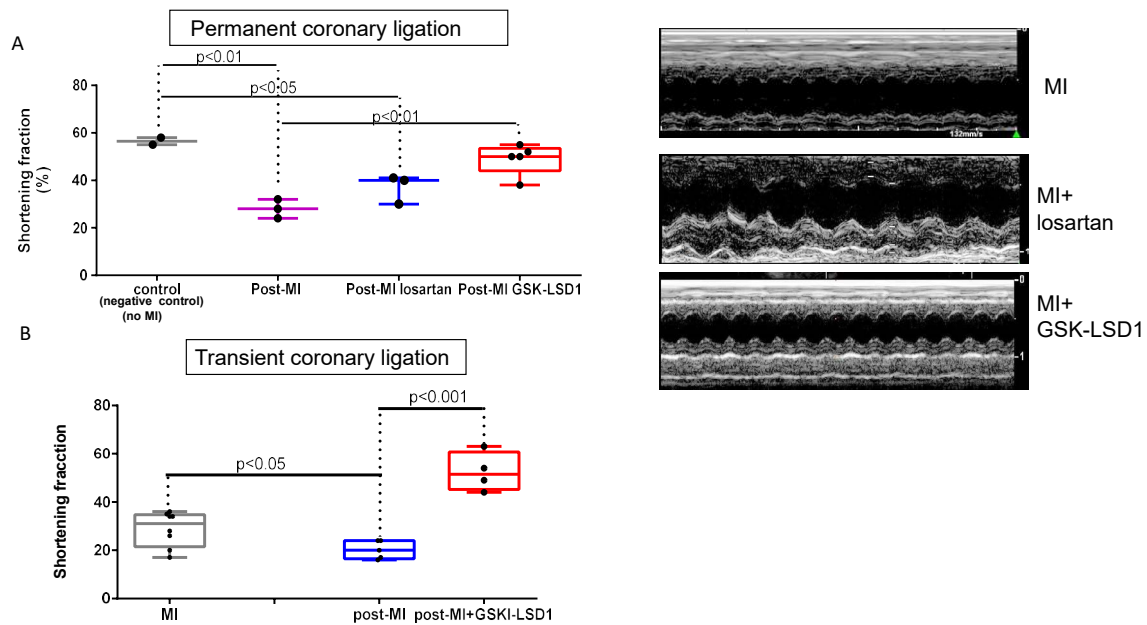
Ventricular function was assessed by echocardiography. Figure 2 shows that the MI-induced decrease in shortening fraction was sligthly but not significantly improved by Losartan while contractility was significantly preserved in GSK-LSD1-treated mice subjected to permanent coronary ligation (Figure 2A). The same beneficial and significant effect of GSK-LSD1 on ventricular function was observed in hearts with transient coronary ligation (Figure 2B).

We further tested whether a process of neo-angiogenesis could occur following the clearing of fibrosis. Heart sections were stained with anti-smooth muscle actin (SMA. SMA+ vessels were scored. Figure S4 illustrates that hearts from MI mice treated with GSK-LSD1 featured much many coronary vessels than hearts from non-treated MI mice.
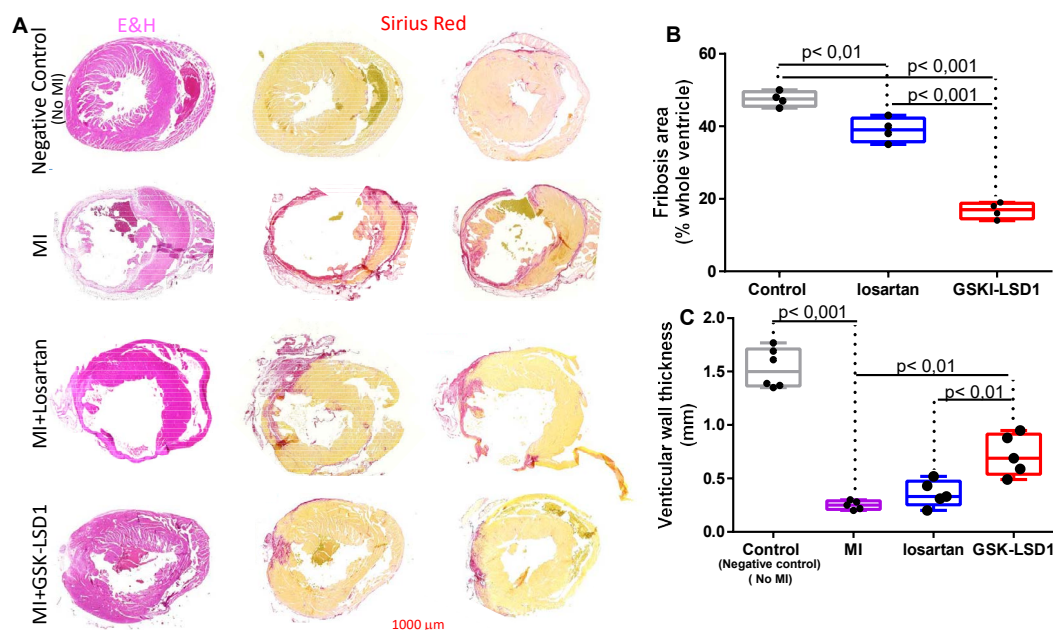
Figure 1: Fibrosis in mouse hearts after myocardial infarction following permanent coronary ligature (A) eosin/hematoxylin (E&H) (left panels) and sirius red (right 2 panels) of heart sections under different experimental conditions, negative controls were healthy mice with no MI and no treatment (B) extent of fibrosis monitored by Sirius red staining and (C) left ventricular wall thickness in MI, losartan- and GSK-LSD1-treated mouse hearts. Significantly different ** p< 0,01,***p<0,001, n=5 mice. Each dot represents a mouse.

Citation: Denis Arnaud, Virginie Lambert, David Benoîst, Amandine Martin, François Roubertie, Jean Gauthier, Michel Pucéat. LSD1 demethylase inhibition prevents cardiac fibrosis in both ischemic and congenital diseases in mice and pig models. Cardiology and Cardiovascular Medicine. 9 (2025): 197-205.

Figure 2: Shortening fraction of mouse hearts under control condition (negative controls are healthy mice with no-MI and no treatment) or after permanent (A) or transient (B) coronary ligation (post-MI). Mice after permanent coronary ligation were treated with losartan (n=4) or GSK-LSD1 (n=5) and mice with transient coronary ligation with GSKLSD1 (n=4). The right panels show some representative echocardiography recordings under the M-mode. Significantly different: *p<0.05, ** p< 0,01,***p<0,001, n=5 mice.

To assess the anti-fibrotic effect of inhibition of LSD1 in a more clinically relevant model, we used a pig model of repaired tetralogy of Fallot which featured right ventricular interstitial fibrosis [18]. Pigs were treated with the inhibitor (1.5 mg/Kg) incorporated in the food 3 weeks (median 21 days) after the surgery for a median duration of 30 days. Echocardiography was performed at the time of euthanasia 6 months post-surgery.

Figure 3 illustrates the extent of fibrosis in non-treated and GSK-LSD1-treated pig hearts. As expected, Sirius red staining was extended over the whole ventricle in non-treated pigs. In contrast, collagen staining was more discrete in GSK-LSD1-treated animals (Figure 3A). The Sirius red staining was confirmed by monitoring the fluorescence emitted by collagen when excited at 560 nm laser in confocal microscopy (Figure 3B). Immunostaining of both periostin, a fibroblast marker and smooth muscle actin (SMA, a marker of myofibroblasts) showed a significant reduction of both cell types in LSD1 inhibitor treated pig right ventricles (Figure 3C). SMA+ cells occupied $44.9 \pm 5\%$ of control heart sections and $2.1 \pm 4\%\%$ of sections from pig hearts treated with GSK-LSD1 (n=3 sections from each pig).
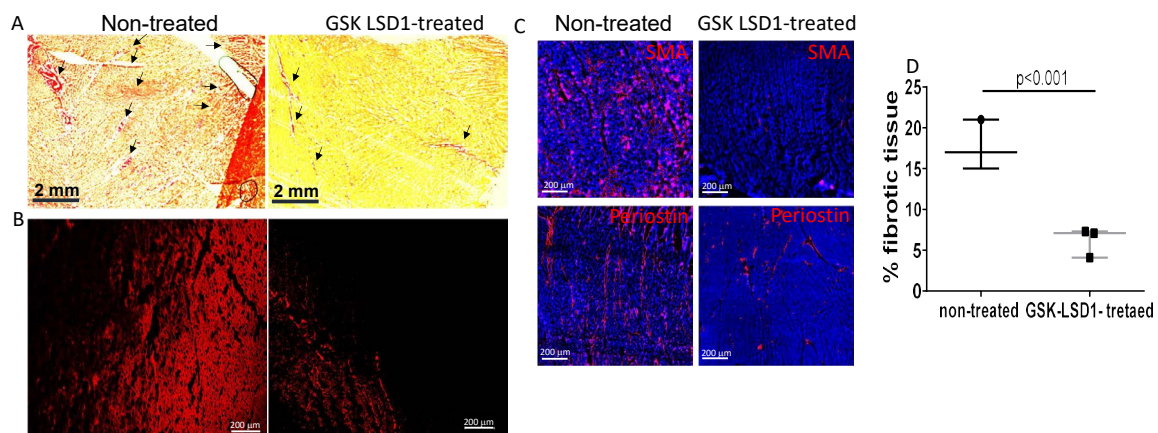
Figure 3: Fibrosis in rTOF pig right ventricle. Cardiac sections from the free wall of the right ventricle from non-treated or GSK-LSD1-treated pigs were stained with Sirius red (A) or collagen fluorescence was imaged using confocal microscopy (B). (C) Cardiac sections were also stained with anti-periostin and anti-smooth actin (SMA) to mark fibroblasts and myofibroblasts. (D) Quantification of collagen monitored by Sirius red staining. The fibrotic area as pointed by arrows in (A) was scored using Image J.

Citation: Denis Arnaud, Virginie Lambert, David Benoîst, Amandine Martin, François Roubertie, Jean Gauthier, Michel Pucéat. LSD1 demethylase inhibition prevents cardiac fibrosis in both ischemic and congenital diseases in mice and pig models. Cardiology and Cardiovascular Medicine. 9 (2025): 197-205.

Interestingly in contrast to mice, we did not observe any neo-angiogenesis in pig hearts treated with GSK-LSD1 (data not shown).

Next, we aimed to evaluate the right ventricular function by echocardiography. The RV/LV diameter ratio showed a dilation of the right ventricle that was less pronounced in GSK-LSD1-treated pig hearts than in non-treated pigs hearts. In the same way, normalized end-diastolic RV diameter and area tended to return to normal values in the treated group without reaching significant differences. The RV wall was significantly less thick in GSK-LSD1-treated heart than in control hearts pointing to less hypertrophy (Figure 4, and supplementary videos).

Changes in normalized TAPSE used to assess global RV dysfunction before, and after development of fibrosis was not significantly and differentially affected in GSK-LSD1-treated pig hearts than in control heart. Nevertheless, on Tissular Doppler imaging, S' wave tended to return to basal values in the treated group. It should be noted that TAPSE reflects only the longitudinal function of the basal RV free wall. Regarding the RV contractility assessed by strain parameters, no difference of the peak global longitudinal strain was observed between the two groups (Figure 4).

Discussion

We found that the treatment with LSD1 inhibitors of both mice following myocardial infarction and pig with right ventricular failure significantly reduced fibrosis. Accordingly, the LSD1 inhibitors significantly improved the recovery of cardiac function after MI in mice. The effect of inhibition of LSD1 in the pig model of repaired tetralogy of Fallot was also significant to prevent the formation of fibrotic interstitial tissue. This resulted in limiting both dilation of the ventricle and hypertrophy of the RV. Although in MI mice treated with LSD1 inhibitor, a neo-angiogenesis was observed, this effect cannot be directly attributed to LSD1 inhibition. Indeed this was not observed in pigs also treated with LSD1 inhibitor. Furthermore, LSD1 itself has been reported to be a HIF1α-dependent pro-angiogenic agent (19). This neo-angiogenesis may rather occur more efficiently in rodents as a secondary process following the clearing of fibrosis.

The treatment of pigs in this pilot study was short (3 weeks) which could have limited its impact. However, LSD1 turns out to be a target to significantly limit the deleterious effect of the right ventricle remodeling and in turn to preserve RV function.
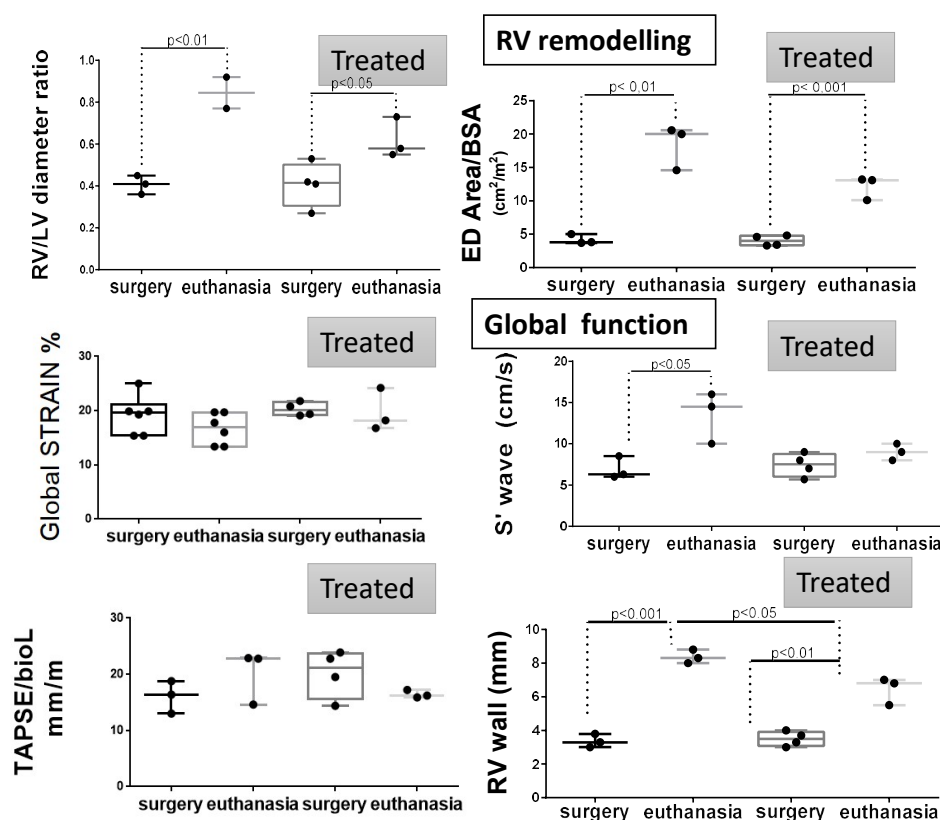
Figures 4: Right ventricular function in pig rTOF. Functional parameters of pigs either non-treated or treated with GSK-LSD1 (Treated) before the surgery (surgery) and at the end point of the experiment (euthanasia). The top graphs reflect the remodeling of the RV and the bottom ones, the function and contractility. The ultrasound images of non-treated (left) or GSK-LSD1- treated pig (right, Treated) show a RV less dilated and with a thinner wall after treatment. Parameters that were monitored are labeled in the y axis of graphs. T-test was used to compare two time points *p<0.05, ** p< 0,01,***p<0,001.

Citation: Denis Arnaud, Virginie Lambert, David Benoît, Amandine Martin, François Roubertie, Jean Gauthier, Michel Pucéat. LSD1 demethylase inhibition prevents cardiac fibrosis in both ischemic and congenital diseases in mice and pig models. Cardiology and Cardiovascular Medicine. 9 (2025): 197-205.

LSD1 inhibitors likely target several cell types within the heart including fibroblasts, activated fibroblasts and macrophages. Indeed, besides cardiomyocytes, it has also been reported that a specific downregulation of LSD1 in Angiotensin II-induced myofibroblasts prevented the intracellular upregulation of transforming growth factor β1 as well as, its downstream effectors Smad2/3, p38, ERK1/2 and JUNK(16). LSD1 inhibition also mediates the anti-fibrotic action of Salsolinol [20]. While required during embryogenesis, low LSD1 activity in adult is increased in cardiac diseases [21], which makes the enzyme an appropriate therapeutic target.

Interestingly LSD1 has also been involved in inflammatory processes through immune cells including macrophages [22-24]. The inflammation is at the origin of fibrosis and the macrophages at the crossroad of such a process [25]. LSD1 inhibitors by targeting several cell types are thus potent modulators of early (i.e. inflammation), middle stage (the EMT process) and late stage (i.e. activation of myofibroblasts) fibrosis.

The molecular mechanism of action of LSD1 inhibitors may be several. LSD1 is together with the REST corepressors (RCORs) the core component of the LSD1/CoREST/HDACs transcriptional repressor complex. It acts at the level of chromatin as a regulator of the transcriptional machinery. The chromatin modifiers complex represses the epithelial or endothelial genes [15] while activating the EMT genes. This explains the pathological effect of LSD1 when reactivated during a pathological situation such as inflammation, cancer or fibrosis including in the heart. Indeed, cardiac fibrosis mainly orginates from epicardial cells and an EMT process which likely leads to new fibroblasts. The latter are further activated into myofibroblasts [26,27].

This however does not exclude another potential effect of LSD1 inhibitor independent from the demethylase activity [28].

LSD1 inhibitors are tested in many clinical trials in oncology [29].These are potent blockers of metastasis which share the process of EMT with fibrosis. EMT is also an active process in the epicardium in diseased atria leading to atrial fibrillation [30]. LSD1 inhibitors could also be considered to prevent the disease. LSD1 inhibitors may turn out to be potent drugs to treat fibrosis in many organs such as kidney an lungs [31-33], two major clinical burden.

Our study together with others [5] reveal that epigenetic modifiers, and more specifically LSD1 inhibitors could be potent drugs for cardiovascular diseases.

Limitations of the study: While the pig model is a faithful model in a clinical situation, it features some limitations; The pigs were treated for only 3 weeks and we could not monitor heart function longer than 2 months later. This is due to the fast growing of these animals which prevents their manipulation when they get over 90 kg, what is their weight 8 months after their surgery to engineer the model.

Supplementary Materials

Figure S1: Individual mouse weight (g) in the course of exper-iments. Figure S2: LSD1 activity in mouse adult heart. Figure S3: extent of fibrosis in left ventricle of post-myocardial infarction (MI) in mice non treated (red square) and mice treated with the reversible LSD1 inhibitor SP-2509. Figure S4: Angiogenesis in post-MI mouse hearts. Videos of RV echocardiography from a non-treated- and a LSD1i-treated pig

Author Contributions

DA carried out the experiments, VL coordinated the pig experiments and performed echocardiography , DB helped in pig experiments, AM performed animal surgeries under the supervision of FR who designed and also performed some pig surgeries. JG funded part of the work and reviewed the manuscript, MP designed the study and wrote the manuscript.

References

1. Collaborators GBDRF. Global burden and strength of evidence for 88 risk factors in 204 countries and 811 subnational locations, 1990-2021: a systematic analysis for the Global Burden of Disease Study 2021. Lancet 403 (2024): 2162-2203.

2. Frangogiannis NG. Cardiac fibrosis. Cardiovasc Res 117 (2021): 1450-1488.

3. Travers JG, Tharp CA, Rubino M, McKinsey TA. Therapeutic targets for cardiac fibrosis: from old school to next-gen. J Clin Invest 132: 2022.

4. Borck PC, Guo LW, Plutzky J. BET Epigenetic Reader Proteins in Cardiovascular Transcriptional Programs. Circ Res 126 (2020): 1190-1208.

5. McKinsey TA, Foo R, Anene-Nzelu CG, Travers JG. Emerging epigenetic therapies of cardiac fibrosis and remodelling in heart failure: from basic mechanisms to early clinical development. Cardiovasc Res 118 (2023): 3482-3498.

6. Alexanian M, Przytycki PF, Micheletti R, Padmanabhan A, Ye L, et al. A transcriptional switch governs fibroblast activation in heart disease. Nature 595(2021) : 438-443.

7. Liu W, Yuan Q, Cao S, Wang G, Liu X, et al. Review: Acetylation mechanisms and targeted therapies in cardiac fibrosis. Pharmacol Res 193 (2023): 106815.

8. Liu ZY, Lin LC, Liu ZY, Yang JJ, Tao H. m6A epitranscriptomic and epigenetic crosstalk in cardiac fibrosis. Mol Ther 32 (2024): 878-889.

9. Lv F, Xie L, Li L, Lin J. LMK235 ameliorates

inflammation and fibrosis after myocardial infarction by inhibiting LSD1-related pathway. Sci Rep 14 (2024): 23450.

10. Aghajanian H, Kimura T, Rurik JG, Hancock AS, Leibowitz MS, et al. Targeting cardiac fibrosis with engineered T cells. Nature 573 (2019): 430-433.

11. Wang J, Du H, Xie W, Bi J, Zhang H, et al. CAR-Macrophage Therapy Alleviates Myocardial Ischemia-Reperfusion Injury. Circ Res 135: 1161-1174.

12. McDonald OG, Wu H, Timp W, Doi A, Feinberg AP. Genome-scale epigenetic reprogramming during epithelial-to-mesenchymal transition. Nat Struct Mol Biol 18 (2011): 867-874.

13. Zhang C, Wang Z, Shi Y, Yu B, Song Y. Recent advances of LSD1/KDM1A inhibitors for disease therapy. Bioorg Chem 134 (2023): 106443.

14. Palumbo-Zerr K, Zerr P, Distler A, Fliehr J, Mancuso R, et al. Orphan nuclear receptor NR4A1 regulates transforming growth factor-beta signaling and fibrosis. Nat Med 21 (2015): 150-158.

15. Guenantin AC, Jebeniani I, Leschik J, Watrin E, Bonne G, et al. Targeting the histone demethylase LSD1 prevents cardiomyopathy in a mouse model of laminopathy. J Clin Invest 131: 2021.

16. Huo JL, Jiao L, An Q, Chen X, Qi Y, et al. Myofibroblast Deficiency of LSD1 Alleviates TAC-Induced Heart Failure. Circ Res 129 (2021): 400-413.

17. Patten RD, Aronovitz MJ, Deras-Mejia L, Pandian NG, Hanak GG, et al. Ventricular remodeling in a mouse model of myocardial infarction. Am J Physiol 274 (1998): H1812-1820.

18. Lambert V, Capderou A, Le Bret E, Rucker-Martin C, Deroubaix E, et al. Right ventricular failure secondary to chronic overload in congenital heart disease: an experimental model for therapeutic innovation. J Thorac Cardiovasc Surg 139 (2010): 1197-1204.

19. Lee JY, Park JH, Choi HJ, Won HY, Joo HS, et al. LSD1 demethylates HIF1alpha to inhibit hydroxylation and ubiquitin-mediated degradation in tumor angiogenesis. Oncogene 36 (2017): 5512-5521.

20. Zhang X, Shao Z, Ni Y, Chen F, Yu X, et al. Salsolinol improves angiotensin II-induced myocardial fibrosis in vitro via inhibition of LSD1 through regulation of the STAT3/Notch-1 signaling pathway. Exp Ther Med 26 (2023): 527.

21. Davis K, Azarcon P, Hickenlooper S, Bia R, Horiuchi E, et al. The role of demethylases in cardiac development

and disease. J Mol Cell Cardiol 158 (2021): 89-100.

22. Yang YT, Wang X, Zhang YY, Yuan WJ. The histone demethylase LSD1 promotes renal inflammation by mediating TLR4 signaling in hepatitis B virus-associated glomerulonephritis. Cell Death Dis 10 (2019): 278.

23. Kim D, Nam HJ, Lee W, Yim HY, Ahn JY, et al. PKCalpha-LSD1-NF-kappaB-Signaling Cascade Is Crucial for Epigenetic Control of the Inflammatory Response. Mol Cell 69 (2018): 398-411.

24. Tan AHY, Tu W, McCuaig R, Hardy K, Donovan T, et al. Lysine-Specific Histone Demethylase 1A Regulates Macrophage Polarization and Checkpoint Molecules in the Tumor Microenvironment of Triple-Negative Breast Cancer. Front Immunol 10 (2019): 1351.

25. Smolgovsky S, Theall B, Wagner N, Alcaide P. Fibroblasts and immune cells: at the crossroad of organ inflammation and fibrosis. Am J Physiol Heart Circ Physiol 326 (2024): H303-H316.

26. Moore-Morris T, Cattaneo P, Puceat M, Evans SM. Origins of cardiac fibroblasts. J Mol Cell Cardiol 91 (2016): 1-5.

27. Tallquist MD, Molkentin JD. Redefining the identity of cardiac fibroblasts. Nat Rev Cardiol 14 (2017): 484-491.

28. Zeng C, Chen J, Cooke EW, Subuddhi A, Roodman ET, et al. Demethylase-independent roles of LSD1 in regulating enhancers and cell fate transition. Nat Commun 14 (2023): 4944.

29. Khan HY, Bajbouj K, Tolba MF. Editorial: Emerging talents in pharmacology of anti-cancer drugs 2022. Front Pharmacol 14 (2023): 1191321.

30. Suffee N, Moore-Morris T, Jagla B, Mougenot N, Dilanian G, et al. Reactivation of the Epicardium at the Origin of Myocardial Fibro-Fatty Infiltration During the Atrial Cardiomyopathy. Circ Res 126 (2020): 1330-1342.

31. Dong L, Yu L, Zhong J. Histone lysine-specific demethylase 1 induced renal fibrosis via decreasing sirtuin 3 expression and activating TGF-beta1/Smad3 pathway in diabetic nephropathy. Diabetol Metab Syndr 14 (2022): 2.

32. Zhang H, Xing J, Zhao L. Lysine-specific demethylase 1 induced epithelial-mesenchymal transition and promoted renal fibrosis through Jagged-1/Notch signaling pathway. Hum Exp Toxicol 40 (2021): S203-S214.

33. Zhang X, Li LX, Yu C, Nath KA, Zhuang S, et al. Targeting lysine-specific demethylase 1A inhibits renal epithelial-mesenchymal transition and attenuates renal fibrosis. FASEB J 36 (2022): e22122.
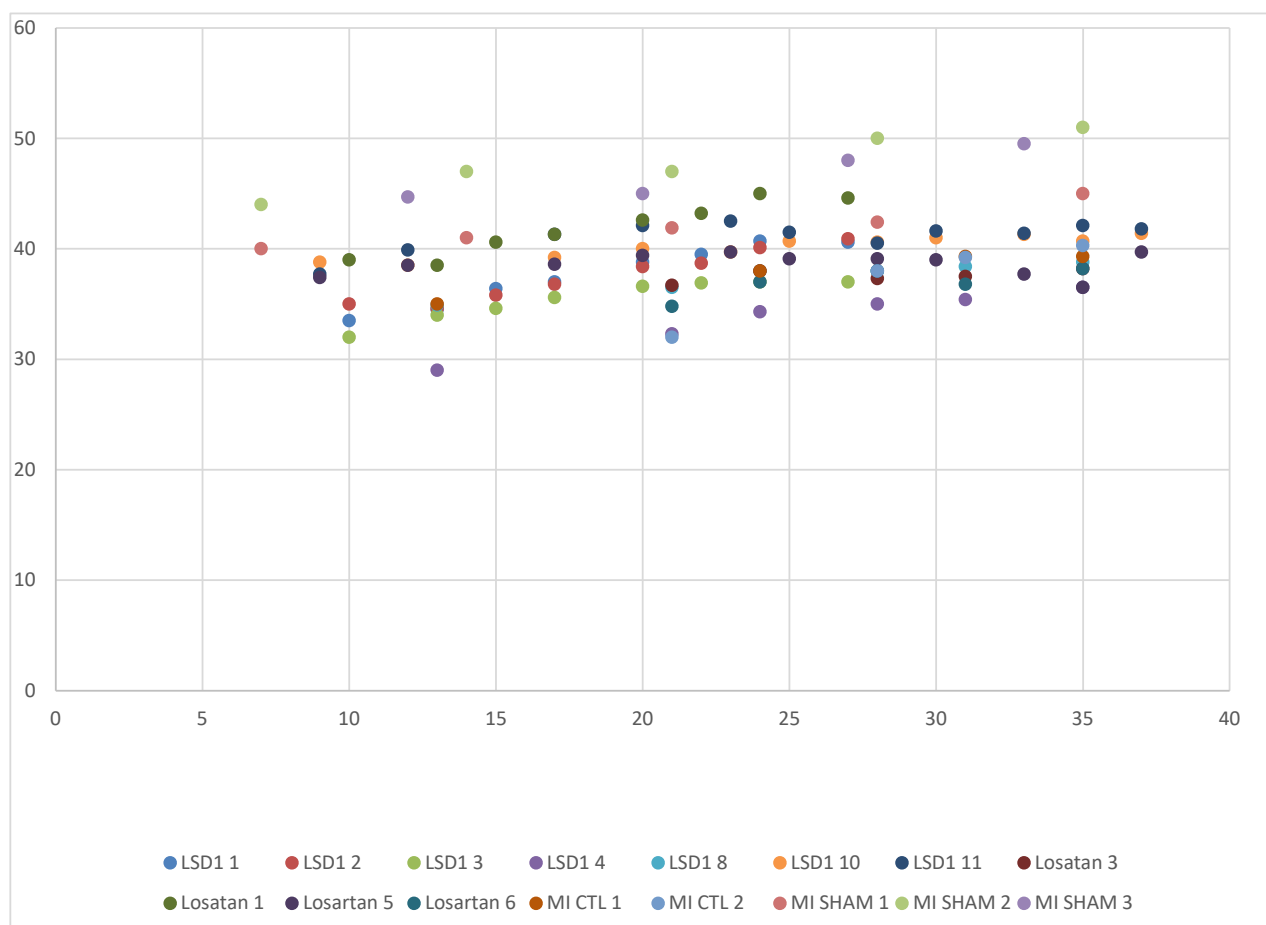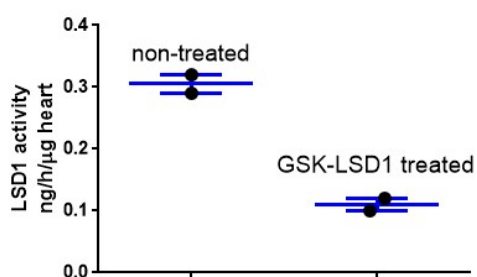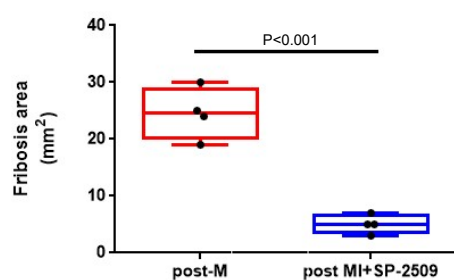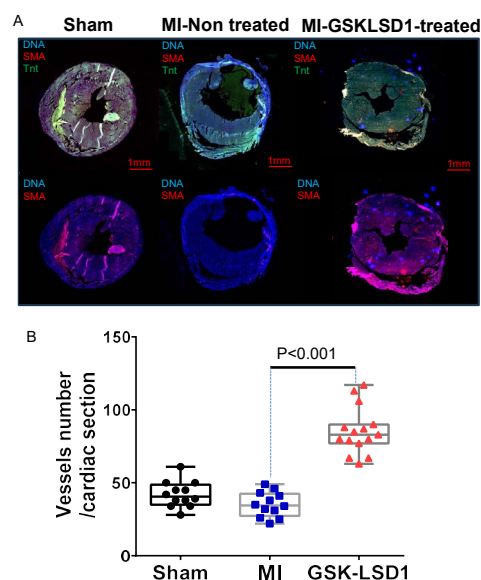
Figure S1: Individual mouse weight (g) in the course of experiments

Figure S2: LSD1 activity in mouse adult heart

Figure S3: extent of fibrosis in left ventricle of post-myocardial infaction (MI) In mice non treated (red square) and mice treated with the reversible LSD1 inhibitor SP-2509

Figure S4: Angiogenesis in post-MI mouse hearts. (A) Cardiac sections(5 sections/heart) of ham, post-MI mousehearts (treated with LSD1 inhibitor) or not (non-treated) were stained with anti-SMA, anti-TnT and dapi (DNA). Images were acquired using a scanner (axioscan Zeiss) at 20X magnification nd Zen= software. (B) SMA+ areas were scored (3 sections hearts, n=4 hearts) using IMARIS software. Two ways anova test: significantly different=p<0.001.

Citation: Denis Arnaud, Virginie Lambert, David Benoîst, Amandine Martin, François Roubertie, Jean Gauthier, Michel Pucéat. LSD1 demethylase inhibition prevents cardiac fibrosis in both ischemic and congenital diseases in mice and pig models. Cardiology and Cardiovascular Medicine. 9 (2025): 197-205.